On the Increasing Fragility of Human Teeth with Age: A Deep-Ultraviolet Resonance Raman Study

J. W. Ager III[a], R. K. Nalla[a,b,†], G. Balooch[a,c], G. Kim[a,b], M. Pugach,[c] S. Habelitz,[c] G. W. Marshall[c], J. H. Kinney[d], and R. O. Ritchie[a,b,*]

[a]Materials Sciences Division, Lawrence Berkeley National Laboratory, Berkeley, CA 94720
[b]Department of Materials Science and Engineering, University of California, Berkeley CA 94720
[c]Department of Preventive and Restorative Dental Sciences, University of California at San Francisco, San Francisco, CA 94143
[d]Department of Mechanical Engineering, Lawrence Livermore National Laboratory, Livermore, CA 94550; UCSF/UCB Joint Graduate Group in Bioengineering, University of California, San Francisco 94143

Author e-mail addresses.

Ager	JWAger@lbl.gov
Nalla	rknalla@gmail.com
Balooch	gbalooch@yahoo.com
Kim	gkim1@uclink.berkeley.edu
Pugach	pugachm@dentistry.ucsf.edu
Habelitz	Stefan.Habelitz@ucsf.edu
Marshall	GW.Marshall@ucsf.edu
Kinney	jhkinney@pacbell.net
Ritchie	RORitchie@lbl.gov

Keywords. Ultraviolet resonance Raman spectroscopy, collagen, dentin, transparent dentin, aging.

***Corresponding author**. Prof. Robert O. Ritchie, Department of Materials Science and Engineering, 216 Hearst Memorial Mining Building, MC 1760, University of California, Berkeley, CA 94720-1760. Tel: (510) 486-5798; Fax: (510) 486-4881. RORitchie@lbl.gov

This work was funded by National Institutes of Health; Division of Materials Sciences and Engineering, Office of Science, U.S. Department of Energy; Laboratory Directed Research and Development Program of Lawrence Berkeley National Laboratory; Guidant Foundation

Running title. Deep-UV Raman study of human teeth

Ms. content. 4857 words, 1 Table, and 6 Figures

[†]current address: Intel Corporation, 5000 W. Chandler Blvd. CH5-159, Chandler, AZ-85226, USA

Conflict of Interest Page

All authors have no conflicts of interest.

MICRO ABSTRACT

Ultraviolet resonance Raman spectroscopy (UVRRS) using 244 nm excitation was used to investigate the impact of aging on human dentin. The intensity of a spectroscopic feature from the peptide bonds in the collagen increases with tissue age, similar to a finding reported previously for human cortical bone.

ABSTRACT

Introduction: The structural changes that lead to compromised mechanical properties with age in dentin and bone are under intense investigation. However, *in situ* analyses of the content and distribution of the mineral phase are more highly developed at present than equivalent probes of the organic phase.

Methods: 35 human molars were divided into three groups: young/normal (23.3±3.8 yr); aged/transparent (74.3±6.0 yr) which had become transparent due to filling of the tubule lumens with mineral deposits; aged/non-transparent (73.3±5.7 yr). Control experiments were performed by demineralizing normal dentin.

Results: Spectral features due to both the amide backbone and resonance-enhanced side chain vibrations were observed. This finding contrasts with reported Raman spectra of proteins in solution excited with similar UV wavelengths, where side chain vibrations, but not strong amide features, are observed. The strong intensity of the amide features observed from dentin is attributed to broadening of the resonance profile for the amide $\pi \rightarrow \pi^*$ transition due to the environment of the collagen molecules in dentin. With increasing age, the height of one specific amide vibration (amide I) becomes significantly higher, when comparing teeth from donors with an average age of 23 years to those of 73 years ($p < 0.001$). This trend of increasing amide I peak height with age is similar to that

previously reported for human cortical bone. The amide I feature also increased in dentin that had been demineralized and dehydrated.

Conclusions: The similar trend of increasing amide I peak height with age in the UVRR spectra of both teeth and bone is surprising, given that only bone undergoes remodeling. However, by considering those observations together with the present study of demineralized/dehydrated dentin and our prior work on dentin dehydrated with polar solvents, a consistent relationship between changes in the UVRR spectra and the collagen environment in the tissue can be developed.

INTRODUCTION

Dentin, the most abundant mineralized tissue in teeth, is a hydrated composite of collagen fibrils and associated non-collagenous proteins, and nanocrystalline apatite. The apatite phase is distributed in two locations: intrafibrallar mineral within or near the gap zones of the collagen fibrils and extrafibrillar mineral between the fibrils [1]. As with bone, the mechanical properties of dentin decline with age; in particular, teeth become more brittle and prone to fracture. This decrease in fracture toughness of dentin with age has been recently established quantitatively by *ex vivo* studies [2,3,4], although precise mechanisms are less certain. For example, there are indications that the mineral content by itself does not determine the elastic properties of hydrated dentin [5].

An effect that occurs naturally with aging is the gradual formation of non-carious (visually) transparent dentin, which starts forming at the apex of the root and sometimes extends into the coronal dentin [6,7,8]. Transparency occurs when a majority of the tubule lumens, which are patent in normal dentin, become filled with mineral. This reduces the refractive index difference between the tubules and the surrounding tissue, thereby decreasing the amount of light scattered off of the lumens. Recently, some specific changes in the mechanical properties of dentin due to age-induced transparency have been clarified. Specifically, transparency was shown to lead to a marked reduction in the inelastic (yielding) behavior and a corresponding deterioration in fracture resistance, which was postulated to be caused by mineral occlusion of the tubule lumens [2]. However, at the same time, transparency did not alter the elastic properties of the intertubular dentin [9]. Subsequent direct examination of the mineral phase at nanometer size-scales, using high-resolution transmission electron microscopy, gave support to the

idea that this filling occurred by a chemical "dissolution and reprecipitation" mechanism [10], akin to that suggested by Daculsi *et al.* [11] for carious dentin.

It is likely that the age-related changes in mineralization patterns in dentin are accompanied by changes in the organic matrix. Type-I collagen is the predominate collagen type in mineralized tissues, and its role in influencing the mechanical properties of bone has been of much recent interest [12,13,14,15,16,17,18,19]. The structure of collagen in mineralized tissues is complex and has hierarchical levels. The collagen molecule is composed of a triple helix, two α_1 chains and one α_2 chain, each of which are approximately 1000 residues long. These molecules then self-assemble into thin (10-300 nm in diameter) collagen fibrils, and often aggregate into large fibers that can be several micrometers in diameter [20]. Within the fibrils, the collagen molecules are staggered by 67 nm and covalently cross-linked between lysine residues which provides its tensile strength [21,22].

Raman spectroscopy, often in combination with other vibrational spectroscopy methods such as Fourier transform infrared (FTIR) spectroscopy, has been used extensively for the study of proteins in aqueous solution. The peak assignments for spectra observed by both methods are well-established and can be divided into vibrations associated with the -CO-NH- bonds that form the peptide backbone and those associated with the side chains of the amino acids. Two vibrations associated with the peptide bonds are strong in visible Raman scattering: amide I (1655-1675 cm^{-1} in solution), which is mostly an in-plane carbonyl stretch, and amide III (1240-1260 cm^{-1} in solution), which involves C-N stretching and N-H bending [23]. The observed frequency of these peaks depends on the secondary structure of the protein (e.g. α-helix, β-sheet, β-turn,

random coil, etc.). For this reason, visible Raman and FTIR spectroscopic methods have been developed for the quantitative evaluation of secondary structure [23,24,25,26].

Ultraviolet excitation can be used to enhance the vibrational intensities of certain parts of proteins through resonance effects [27,28,29]. In ultraviolet resonance Raman (UVRR) spectroscopy, excitation wavelengths near 200 nm can be used to selectively enhance the intensity of the amide I vibration via its $\pi \rightarrow \pi^*$ transition [30], while excitation at longer wavelengths in the 230-250 nm range selectively enhances features due to the side chains of aromatic amino acids [27,31]. Excitation in this range also increases the intensity of the amide II feature (ca. 1560 cm^{-1}, N-H bending and C-N stretching) [27]. Deep ultraviolet excitation has been used to probe structure changes caused by binding events [32], and to study hydration of collagen I in solution [33].

There are far fewer Raman studies of proteins in solid media such as teeth and bone [34]. The visible and near-IR Raman spectrum of human bone has strong features due to both organic and inorganic (hydroxyapatite) components. For this reason, Raman spectroscopy and microspectroscopy have been used to study the effects of aging and disease on bone mineralization [35], to evaluate the strain born by the inorganic component under mechanical deformation [36,37,38], and to study mineral distributions with near-micron spatial resolution [39]. It should be noted, however, that a specific challenge of applying visible Raman spectroscopy to solid tissues is fluorescence interference [40], leading to the use of near-IR excitation [41,42] and sophisticated background subtraction and data analysis techniques [39] to mitigate this effect.

Recently, we reported the first *in situ* UVRRS measurements of human cortical bone and found age-induced changes in the amide I band [43]. Here, we apply the same

technique to human teeth to determine if similar trends with aging are observed and to elucidate their origin. We found that the height of the resonance-enhanced amide I peak in dentin, as in bone, increases with age. This result is surprising as, unlike bone, dentin does not undergo remodeling. We also observed that in teeth from older donors, the UVRR spectra are not much altered by the degree of transparency, which implies that the intrafibrallar collagen environment is not significantly affected by the accumulation of nanocrystalline mineral within the tubule lumens, which are usually occupied by odontoblastic processes.

MATERIALS AND METHODS

Specimen preparation

Human molars, recently extracted according to protocols approved by the University of California, San Francisco Committee on Human Research, were used in this study. The sample matrix is summarized in Table 1. A total of 35 teeth were used and were divided into three groups, henceforth referred to as *young/normal* (N = 10, 23.3±3.8 yr), *aged/non-transparent* (N = 12, 73.3±5.7 yr), and *aged/transparent* (N = 13, 74.3±6.0 yr). This choice of groups was made with the intention of additionally evaluating whether the process of dentin transparency has an effect on the UV-Raman spectrum of teeth. Beams (~1 x 1 x 11 mm; one per tooth) were sectioned from the central portion of the crown and the root vertically through the teeth using a low speed diamond saw. Examined surfaces were wet-polished to a 1200 grit finish. Specimens were kept hydrated in Hanks' Balanced Salt Solution (HBSS) throughout preparation and testing. Demineralization studies were performed on 2-mm-thick occlusal dentin disks prepared from teeth in the young/normal group using 10% citric acid with exposure times between 15 sec and 24 hr.

Citric acid is used as an etchant for adhesive bonding to dentin and its etching rate has been studied quantitatively in a prior study [44]. Hydrated type I collagen membranes (from bovine Achilles tendon; Ace Surgical Supply) were used as a comparison standard for fully demineralized tissue.

Ultraviolet Resonance Raman Spectroscopy

The UV Raman system incorporated a continuous wave (cw) intracavity doubled argon ion laser, which provided the excitation at 244 nm; a filter was used to remove plasma lines. The laser was focused to a ~500 μm spot on the surface of the samples by a *f*/4 100 mm fused silica lens. Back-scattered light was collimated by the same lens and directed to a UV-optimized triple spectrometer equipped with a liquid-nitrogen-cooled, back-thinned, CCD detector. Further details can be found elsewhere [43].

Care was taken to eliminate effects due to damage to the samples caused by UV exposure. Specimens were mounted on a rotating stage; the pure collagen samples were pressed flat and mounted on the same stage. The laser power at the sample was below 5 mW, and the CCD was operated in multiple frame mode. Comparison of sequential data frames allowed experimental conditions to be developed under which spectra did not change over the experimental time period. A typical protocol was 3 frames of 30 sec duration each. The instrument dispersion corresponded to 2.1 cm^{-1}/pixel; this dispersion is smaller than what is typically employed in visible Raman studies due to the compression of the Raman spectrum in wavelength space (4 times the spectral precision is required for equivalent Raman shift resolution for 244 nm as compared to 488 nm excitation.). The instrument resolution was varied between 15 cm^{-1} and 30 cm^{-1} by adjusting the slit width of the dispersion stage of the triple spectrometer. These

measurements established that the linewidths of the major features in the spectrum, e.g., of the well-resolved CH_2 wag, were 40 cm^{-1} and higher. Data were obtained at 30 cm^{-1} instrument resolution to maximize sensitivity without artificially broadening the lines. The data frames were averaged and a small linear background was defined by the signal at 500 and 2000 cm^{-1} (where little Raman scattering from the sample is expected) and subtracted. Presented spectra were normalized to the height of the CH_2 wag peak at ~1460 cm^{-1}.

Statistical Analysis

The means within the groups were evaluated either by Student's *t* test (for comparing the old/non-transparent and old/ transparent groups) or ANOVA (when comparing all three groups). A *p* value of less than 0.05 was considered significant.

RESULTS

UVRR spectra and peak assignments

Figure 1 shows typical Raman spectra of dentin from the three groups in the study. With the exception of the aromatic side chain features (discussed below), peak assignments are made based on prior visible and near-IR Raman spectra of bone [34]. The peak near 960 cm^{-1} is assigned to the ν_1 motion of the PO_4^{3-} in the apatite mineral. The features at ca. 1250 cm^{-1} and 1460 cm^{-1} are assigned to the amide III vibration of the peptide bonds and the CH_2 wag bands of collagen I. As we found previously for a study of human bone from donors over a similar age range [43], the region of the UVRR spectrum between 1200 and 1500 cm^{-1} did not vary significantly between different samples.

We thus concentrated our analysis on the region of the spectra that showed the largest variance between samples, namely that from 1500 to 1800 cm^{-1}. In the visible Raman spectrum of bone, amide II (ca. 1560 cm^{-1}) and amide I (ca. 1660 cm^{-1}) are assigned in this spectral region. We have shown previously that compared to visible excitation, features due to the organic phase are stronger compared to the mineral phase when 244 nm excitation is used [43]. For example, the PO_4^{3-} ν_1 feature is dominant in visible and near-IR spectra of mineralized tissues; when UV excitation is used, this feature is weak compared to the amide features. Thus, it is very likely that the strong intensity of the features in the vicinity of the amide vibrational frequencies is due to a resonance Raman effect. Figure 2 compares the UVRR spectrum of human dentin excited at 244 nm with a spectrum from hydrated gel-like type-I collagen without mineral, a spectrum from solution phase collagen excited at 229 nm [33] and from solution-phase myoglobin excited at 205 nm. Evidently, 244 nm excitation leads to resonance enhancement of the amide I feature (ca. 1660 cm^{-1}) which is dominant in the spectrum from the transparent molar and observable in the gel-like collagen. In solution, enhancement of the amide I feature requires shorter wavelength excitation (near 200 nm) to be in resonance with the amide $\pi \rightarrow \pi^*$ transition. The amide II feature (1560 cm^{-1}) may also have a resonance effect, although this feature is visible in all four spectra shown in Fig. 2.

There is a shoulder near 1620 cm^{-1} on the amide I feature of dentin and hydrated gel-like collagen [Fig 3(a) and (b), Fig 2(b)]. The frequency of this feature corresponds to a peak that is assigned to the Y8a tyrosine side chain vibration in the UVRRS of solution-phase collagen. We thus assign the peak at 1660 cm^{-1} in our UVRR spectra to amide I and its low frequency shoulder to Y8a. We realize that trytophan and phenylalanine also

have ring-breathing vibrations near Y8a, but based on the assignment used by Juszczak [33] and on the low levels of trytophan in collagen, we feel that it is likely that most of the spectral intensity comes from Y8a. Based on these assignments, non-linear least-squares fitting was used to extract the heights of the overlapping 1580 cm^{-1} (amide II), 1610 cm^{-1} (Y8a), and amide I (1660 cm^{-1}) bands. Our curve-fitting approach is similar to that of Malti *et al.* [26], except that we do not find it necessary to include a high-frequency amide I component for spectra excited at 244 nm. Example fits are shown in Figure 3.

UVRR spectra of hydrated dentin specimens from the young/normal sample group that were demineralized by exposure to citric acid are shown in Fig. 4(a) for specimens that were kept hydrated after demineralization. It can be seen that the PO_4^{3-} ν_1 peak at ca. 960 cm^{-1} is present in dentin exposed for 1 min but absent for exposures of 30 min and longer. This observation is consistent with prior kinetic measurements of demineralization of dentin with 10% citric acid [44] which found that 15 second exposures can demineralize dentin to a depth of 700 nm and that the depth of demineralization depends on the square root of time. Given the small penetration depth of the laser, which cannot be more than a few 100 nm and is probably much shallower, we can assume that exposures of 30 min and longer fully demineralize (extrafibrallar and intrafibrallar) the dentin in the near-surface volume sampled by UV Raman scattering. As shown in the inset, the height of the amide I peak remains relatively constant in hydrated dentin as a function of citric acid exposure time. Similar behavior was observed in this sample for Y8a.

As shown in Fig. 4(b), in young/normal dentin that was allowed to dry after citric acid exposure, the height of the overlapping Y8a/amide I peak was increased, as compared to the untreated control sample. Peak fitting revealed that most of this increase was due to an increase in the amide I peak height (inset). The effect of dehydration was reversible (Fig. 5); that is, in a sample for which citric acid exposure and dehydration increased the height of the Y8a/amide I peak, rehydration caused the peak to be reduced back to near its initial intensity. As a control experiment, the effect of citric acid exposure on hydrated, unmineralized type 1 collagen from bovine tendon was investigated. No significant differences were found between the spectra at any of the demineralization time points and the spectrum of untreated hydrated collagen, which is shown in Fig. 2(b). This indicates that citric acid exposure does not have a direct effect on collagen.

Statistical analysis

The peak widths observed here are somewhat broader than those observed by UVRR spectroscopy for solution-phase proteins including collagen [33]. The amide features in spectra obtained with 15 cm^{-1} spectral resolution were not significantly narrower compared to spectra taken with 30 cm^{-1} resolution, suggesting that that the line shapes are not instrument-limited. We attribute the broad lines to the inhomogeneous broadening caused by the heterogeneous environment of collagen in dentin compared to collagen in solution. The broadening creates some uncertainty in the precise peak position. Based on the range of values obtained for relatively sharp, non-overlapping features such as the phosphate peak and the CH_2 wag, this uncertainty is about ± 5 cm^{-1} (this corresponds to 2.5 pixels on the detector). Thus we concentrated on determining the peak heights of the

major spectral features, which can be reliably determined from the spectra; these were correspondingly used for statistical analysis.

The height of the CH_2 wag did not vary significantly between the three dentin sample groups (ANOVA). The amide I peak height varied considerably between sample groups. The peak heights for the Y8a and amide I features for the three groups of dentin (Normal, Old/Non-transparent, and Old/Transparent) evaluated in this study are shown in Fig. 6(a). The Y8a and amide I peak heights from five demineralization experiments: two performed hydrated, one performed after hydration, and one with data from hydrated and dehydrated samples form the same run are summarized in Fig. 6(b). The control values represent the means of the unexposed dentin used in this study. Data from dentin demineralized for 30 min and longer (c.f., Fig. 4) were used to form the "wet" and "dry" sample sets. Also shown are peak height data from our prior study on human cortical bone as a function of age [43].

In the dentin data set, we did not observe a significant difference in the Y8a peak height between groups (ANOVA, $p > 0.10$) or for the two older sample sets compared to young/normal. However, the amide I peak height was significantly different (t test, $p < 0.001$) between both of the older data sets and the young/normal set [Fig. 6(a)]. The amide I feature was not significantly different between the aged/non-transparent and aged/transparent groups (t test, $p > 0.10$). Referring to Fig. 6(b), demineralization produces a significant increase in the amide I peak height after dehydration, but not if the samples are kept hydrated. The Y8a feature decreases compared to the control; this trend was significant ($p < 0.05$) in the wet sample set.

DISCUSSION

We find that the largest observable difference between the UVRR spectra taken in this study is the height of the amide I feature, although we will discuss smaller changes in the spectra below. It is surprising that the amide I feature is observed at all with excitation at 244 nm. In solution, excitation closer to 200 nm is generally required to enhance this feature via its $\pi \rightarrow \pi^*$ transition [27,30,31]. Moreover, the amide I feature is not observed in solution phase spectra obtained with 244 nm excitation in myoglobin [32] or cytochrome c oxidase [29], or with 229 nm excitation in collagen [33]. This is consistent with the UV absorption spectrum of collagen, which has a maximum due to the $\pi \rightarrow \pi^*$ transition at 190 nm ($\varepsilon = 8\text{x}10^{-3}$) and little absorption ($\varepsilon < 1\text{x}10^{-4}$) for $\lambda > 235$ nm [45]. In contrast, in the solid-phase for both dentin and cortical bone the amide I feature is the strongest feature in the UVRR spectrum. Evidently, the resonance enhancement profile of amide I is broadened significantly by the collagen environment in mineralized tissues.

However, the environment of the collagen molecules in solid matrices such as dentin and bone also produces inhomogeneous broadening of the spectral features. This can be seen by comparing the spectra of dentin and solution-phase collagen shown in Fig. 2 (solution phase proteins have even narrower features [29]). As discussed above, this produces uncertainties in the determination of the precise peak position, thus ruling out the application of confirmational analyses developed for the solution phase that are based on small shifts in the amide III and amide I features [24] and those developed for analyzing strained collagen [46] and bone [37,38] which are also based on small peak shifts. It also limits analysis of some of the weaker observed features. For example, a

weak peak near 1750 cm^{-1} was observed in some spectra (e.g., two of the spectra in Fig. 1). Also, the amide I frequency was not always symmetric to higher frequency, suggesting additional intensity near 1680 cm^{-1}. Peaks in both these spectra regions were employed in the devolution of the amide I peak in the FTIR study of collagen in bone by Paschalis *et al.* [12] and used to quantify the degree of cross-linking. Here, due to the broad nature of the main amide I feature, these features were not consistently observed with sufficiently high signal-to-noise to develop quantitative analyses based on their intensity.

We base our analysis on the intensity of the strongest features in the spectra that were observed to vary significantly between samples. As shown in Figs. 1, 3, and 4(b), the intensity of the amide I peak can change by factors of at least 2. Actually, the weaker amide II feature also showed similar trends as amide I, but since its intensity was correlated with that of amide I (r = 0.55) in the dentin sample set, we did not consider it an independent measure. The amide III feature did not vary significantly between the samples. The differences in behavior between the three observed amide features is not surprising given that they have different transition dipoles and show different resonance Raman behaviors in solution [27]. We choose to include Y8a in our analysis because it could be expected that the resonance enhancement of this side-chain vibration in mineralized tissues might be quite different from that of vibrations associated with the peptide bonds (e.g., the amide modes). It should be noted that we cannot exclude a contribution to the UVRR spectra of dentin and bone from non-collagenous proteins. However, given the magnitude of the changes in the amide I peak (as high as a factor of

2), we think it unlikely that changes to a component that is <10% of the total protein content of the tissues could produce a significant fraction of the observed effects.

When dentin is demineralized by acid exposure, apatite mineral is dissolved and water or acid occupies the space formerly occupied by the mineral. In the course of dentin demineralization, mineral is removed first from the extrafibrillar compartment, and the intrafibrillar mineral is removed last since it is protected by the collagen [47]. In completely demineralized dentin, water molecules are able to enter the fibril. If demineralized dentin is dehydrated, the surface collapses and the collagenous matrix shrinks until it is supported by the partially or completely mineralized dentin below it [48,49,50]. For more complete demineralization, we expect a more complete collapse of the intertubular demineralized dentin matrix [51].

This picture of the demineralization process is supported by mechanical and structural studies [51,52,53,54]. For example, analysis of hydrated and dehydrated dentin collagen revealed that dehydration affects fibril diameter and repeat distance in a reciprocal way [55]. Tapping mode images obtained with atomic force microscopy (AFM) showed significant differences in the distribution of fibril diameter and axial repeat distance, depending on the hydration state of the substrate. After dehydration the periodicity shortened for some fibrils and showed an overall wider distribution. According to some studies, hydrated fibrils have a higher degree of structural organization, while dehydration causes structural disorder and mechanical stresses. Upon dehydration, loss of adsorbed and chemically bound water molecules destabilizes the quaternary structure of collagen molecules and lowers the degree of organization in the fibril [56,57,58].

The present Raman data are consistent with this picture. The stability of the Raman spectra in hydrated, demineralized dentin and the reversible changes in the Raman spectra with hydration/dehydration (Fig. 5) are consistent with the idea that water can support the collagen structure, even after both the intrafibrallar and extrafibrallar mineral are removed. This is also consistent with the recent observation of a structured layer of water between the mineral and organic phases of bone [59]. The presence or absence of mineral (even intrafibrallar mineral) therefore does not have a direct effect on the amide I peak intensity. On the other hand, other perturbations of the collagen environment, as produced by dehydrating demineralized dentin or, as reported previously, by exposing dentin to non-physiological solvents such as ethanol and acetone [60], clearly increase the amide I intensity. Based on the physical model for demineralization presented above, we would expect, and in fact observe, an increase in the amide I peak height in dehydrated and demineralized dentin, because of the increased interaction between collagen fibrils caused by stretching and intrafibrillar movement. We would also expect that increased mineralization in the tubule lumens in transparent dentin would have little effect, which is what was observed. Finally, we note that the Y8a peak decreases in hydrated demineralized dentin suggesting that the Y8a intensity may be specifically affected by intrafibrallar mineral; however, we regard this finding as tentative.

We now turn to the finding that the height of the resonance-enhanced amide I feature increases with increasing age in dentin and bone, which suggests that similar changes in the collagen environment may be occurring in both mineralized tissues. It is well established that the density of bone on the macroscopic scale decreases with age due to natural processes and to bone metabolic diseases such as osteoporosis; however, the

density of mineral per unit volume of bone, excluding porosities, actually increases [61]. At the fibril level, this is due to increased mineralization [62], with higher crystallinity [63]. While the dentin demineralization data have established that intrafibrallar mineral does not have a direct effect on the amide I resonance, there may be associated changes, similar to those induced by dehydration, that occur as a result of aging. These might be increased local stresses or increases in structural disorder of the fibrils.

It is useful to examine this hypothesis in light of the small angle x-ray scattering and transmission electron microscopy data obtained from dentin [2,10]. In these studies, it was found that the average mineralization increased in transparent dentin, while at the same time, the crystallite size decreased. An increase in mineral density, accompanied by a decrease in crystallite size, would accommodate a higher packing density in the transparent dentin. We consider it possible that the packing density of the mineral crystallites affects the amide resonance.

It is important that the amide I peak increases with age in both teeth and bone, implying that some (not necessarily the same) physical change in both tissues broadens the amide resonance Raman excitation profile. This finding is surprising in light of the fact that unlike teeth, bone undergoes constant remodeling with age. It is possible that the trend in both tissues is driven by the increase of density with age that is known to occur in both tissues. Increased cross-linking in bone [41] and dehydration in dentin, the latter leading to increased inter-collagen hydrogen bonding [42], could be the possible mechanisms, although further study is clearly required.

It is interesting to note that in bone the amide I peak increases with age while the fracture toughness declines, whereas in dentin dehydrated with solvents, the peak height

also increases, but the fracture toughness does as well [60], i.e., for the same changes in the Raman spectra, one observes remarkably different mechanical behavior in teeth versus bone. Such changes in the amide I peak have been associated with increased stiffness in both mineralized tissues; however, as there is no simple direct relationship between elastic modulus and resistance to fracture, it is not immediately obvious how such changes in stiffness affect the toughness. For example, increased stiffness with drying leads to lower fracture toughness in both dentin and bone, while the same magnitude of increased stiffness that results from exposure to alcohol produces higher fracture toughness.

In summary, ultraviolet resonance Raman spectroscopy with 244 nm excitation was used to obtain spectra from human dentin, specifically in the young/normal (mean age 23.3 yrs), aged-non-transparent (mean age 73.3 yrs), and aged-transparent (mean age 74.3 yrs) conditions. The observed spectra contain resonance enhanced features from both amino acid side chains (Y8a) and from the amide I and amide II motions of the peptide bonds of type I collagen. The appearance of resonance-enhanced amide features at a wavelength much longer than typically used in solution phase work (200 nm) is due to broadening of $\pi \rightarrow \pi^*$ amide resonance produced by the environment of the collagen. The height of the amide I feature was significantly different ($p < 0.001$) between the "normal" and the combined "aged-transparent" and "aged" data sets, which is a finding similar to what was found earlier in human cortical bone. Analysis of spectral changes produced by demineralizing and dehydrating dentin was used to elucidate the nature of the structural changes in dentin that produce the observed effects. The factors responsible for age-induced changes in the UVRR spectra of dentin and bone are likely to be increased tissue

density, due to increased density of the mineral phase (for bone and teeth) and to dehydration (for teeth).

ACKNOWLEDGEMENTS

This work was supported by the National Institutes of Health under Grants No. 5R01 DE015633 (for RKN) and P01DE09859 (for JHK SJM, GWM), by the Director, Office of Science, Office of Basic Energy Sciences, Division of Materials Sciences and Engineering, Department of Energy (for JWA, ROR) and by the Laboratory Directed Research and Development Program of Lawrence Berkeley National Laboratory (for GB) under contract No. DE-AC02-05CH11231. GK was supported by the Guidant Foundation Summer Undergraduate Research Program. We acknowledge Ms. Grace Nomomura for maintaining the documented tooth collection from which the samples were selected.

REFERENCES

1. Landis WJ, Hodgens KJ, Arena J, Song MJ, McEwen BF 1996 Structural relations between collagen and mineral in bone as determined by high voltage electron microscopic tomography. Microsc Res Tech **33**:192-202.
2. Kinney JH, Nalla RK, Pople JA, Breunig TM, Ritchie RO 2005 Age-related transparent root dentin: mineral concentration, crystallite size, and mechanical properties. Biomaterials **26**:3363-76.
3. Arola D, Reprogel RK 2005 Effects of aging on the mechanical behavior of human dentin. Biomaterials **26**:4051–4061.
4. Bajaj D, Sundaram N, Nazari A, Arola D 2006. Age, dehydration, and fatigue crack growth in dentin. Biomaterials **27**: 2507-2517.
5. Kinney JH, Habelitz S, Marshall SJ, Marshall GW 2003 The importance of intrafibrillar mineralization of collagen on the mechanical properties of dentin. J Dent Res. **82**:957-961.

6. Micheletti Cremasco M. 1998 Dental histology: study of aging processes in root dentine. Boll Soc Ital Biol Sper **74**:19-28.

7. Vasiliadis L, Darling AI, Levers BG 1983 The amount and distribution of sclerotic human root dentine. Arch Oral Biol **28**:645-649.

8. Vasiliadis L, Darling AI, Levers BG 1983 The histology of sclerotic human root dentine. Arch Oral Biol **28**:693-700.

9. Balooch M, Demos SG, Kinney JH, Marshall GW, Balooch G, Marshall SJ 2001 Local mechanical and optical properties of normal and transparent root dentin. J Mat Sci: Mater in Med **12**:507-514.

10. Porter AE, Nalla RK, Minor A, Jinschek JR, Kisielowski C, Radmilovic V, Kinney JH, Tomsia AP, Ritchie RO 2005 A transmission electron microscopy study of mineralization in age-induced transparent dentin. Biomaterials **26**:7650-60.

11. Daculsi G, LeGeros RZ, Jean A, Kerebel B 1987 Possible physico-chemical processes in human dentin caries. J Dent Res **66**:1356-1359.

12. Paschalis EP, Verdelis K, Doty SB, Boskey AL, Mendelsohn R, Yamauchi M 2001 Spectroscopic characterization of collagen cross-links in bone. J Bone Miner Res. **16**:1821-8.

13. Paschalis EP, Shane E, Lyritis G, Skarantavos G, Mendelsohn R, Boskey AL 2004. Bone fragility and collagen cross-links. J Bone Miner Res **19**:2000-4.

14. Bailey AJ, Sims TJ, Ebbesen EN, Mansell JP, Thomsen JS, Mosekilde L 1999. Age-related changes in the biochemical properties of human cancellous bone collagen: relationship to bone strength. Calcif Tissue Int **65**:203-210.

15. Oxlund H, Mosekilde K, Ørtoft G 1996. Reduced concentration of collagen reducible cross links in human trabecular bone with respect to age and osteoporosis. Bone **19**:479-484.

16. Zioupos P, Currey JD, Hamer AJ 1999. The role of collagen in the declining mechanical properties of aging human cortical bone. J Biomed Mater Res. **2**:108-116.

17. Wang X, Bank R, Tekoppele J, Agrawal C 2001 The role of collagen in determining bone mechanical properties. J Orthop Res **19**:1021-1026.

18. Wang X, Shen X, Li X, Agrawal CM. 2002. Age-related changes in the collagen network and toughness of bone. Bone **31**:1-7.

19. Wang X, Li X, Shen X, Agrawal CM 2003 Age-related changes of noncalcified collagen in human cortical bone. Ann Biomed Eng. **31**:1365-1371.

20. Veis A 1997 Collagen fibrallar structure in mineralized and nonmineralized tissues. Current Opinion in Sol. State Mat Sci:**2**:370-8.

21. Eyre DR, Paz MA, Gallop PM 1984 Cross-linking in collagen and elastin. Annual Rev Biochem **53**:717-748.

22. Knott L, Bailey AJ 1998 Collagen cross-links in mineralizing tissues: A review of their chemistry, function, and clinical relevance. Bone **22**:181-187.

23. Tu AT 1986 Peptide Backbone Confirmation and Microenvironment of Protein Side Chains.In: Clark RJH, Hester RE (ed.) Spectroscopy of Biological Systems, Wiley, New York, pp. 47-111.

24. Sane SU, Cramer SM, Przybycien TM 1999 A holistic approach to protein secondary structure characterization using amide I band Raman spectroscopy. Anal Biochem **269**:255-272 and references therein.

25. Pelton JT, McLean LR 2000 Spectroscopy Methods for Analysis of Protein Secondary Structure. Anal Biochemistry **277**:167-176.

26. Malti NC, Aperti MM, Zagorski MG, Cary PR, Anderson VE 2004 Raman spectroscopic characterization of secondary structure in natively unfolded proteins: α-synuclein. J Amer Chem Soc **126**:2399-2408.

27. Harada I, Takecuhi H 1986 Raman and Ultraviolet Resonance Raman of Proteins and Related Compounds. In: Clark RJH, Hester RE (ed.) Spectroscopy of Biological Systems, Wiley, New York, NY, pp. 113-175.

28. Asher SA 2002 Ultraviolet Raman spectroscopy. in Handbook of Vibrational Spectroscopy – Theory and Instrumentation. Wiley, New York, NY, vol. 1, pp. 557-571.

29. Aki M, Ogura T, Shinzawa-Itoh K, Yoshikawa S, Kitagawa T 2000 A new measurement system for UV resonance Raman spectra of large proteins and its application to Cytochrome *c* oxidase. J Phys Chem B **104**:10765-10774.

30. Mikhonin AV, Ahmed Z, Ianoul A, Asher SA 2004 Assignments and conformational dependencies of the Amide III peptide backbone UV resonance Raman bands. J Chem Phys B **108**:19020-19028.

31. Chi Z, Chen XG, Holtz JSW, Asher SA 1998 UV resonance Raman-selective amide vibrational enhancement: quantitative methodology for determining protein secondary structure. Biochemistry **37**, 2854-2864 and references therein.

32. Haruta N, Aki M, Ozaki S-I, Watanabe Y, Kitagawa T 2001 Protein confirmation change of myoglobin upon ligand binding probed by ultraviolet resonance Raman spectroscopy. Biochemistry **40**:6956-6963.

33. Juszczak LJ 2004 Comparative vibrational spectroscopy of intracellular tau and extracellular collagen I reveals parallels of gelation and fibrillar structure. J Biol Chem **279**:7395-7404.

34. Carden A, Morris MD 2000 Application of vibrational spectroscopy to the study of mineralized tissues (review) J Biomed Opt **5**:259-268 and references therein.

35. Akkus O, Adar F, Schaffler MB 2004 Age-related changes in physicochemical properties of mineral crystals are related to impaired mechanical function of cortical bone. Bone **34**:443-53.

36. Pezzotti G, Sakakura S 2003 Study of the toughening mechanisms in bone and biomimetic hydroxyapatite materials using Raman microprobe spectroscopy. J Biomed Mater Res A **65**:229-236.

37. Carden A, Rajachar RM, Morris MD, Kohn DH 2003 Ultrastructural changes accompanying the mechanical deformation of bone tissue: a Raman imaging study. Calcif Tissue Int. **72**:166-75.

38. Morris MD, Finney WF, Rajachar RM, Kohn DH 2004 Bone tissue ultrastructural response to elastic deformation probed by Raman spectroscopy. Faraday Discuss. **126**:159-168.

39. Timlin JA., Carden A., Morris MD, Bonadio JF, Hoffler II CE, Kozloff KM, Goldstein SA 1999 Spatial distribution of phosphate species in mature and newly generated mammalian bone by hyperspectral Raman imaging. J. Biomed. Optics. **4**:8-34.

40. Freeman JJ, Silva MJ 2002 Separation of the Raman spectral signatures of bioapatite and collagen in compact mouse bone bleached with hydrogen peroxide. Appl. Spectros. **56**:770-775.

41. Kontoyannis CG, Vagenas NV 2000 FT-Raman spectroscopy: a tool for monitoring the demineralization of bones. Appl. Spectros. **54**:1605-1609.

42. Lakshmi RJ, Alexander M, Kurien J, Mahato KK, Kartha VB 2003 Osteoradionecrosis (ORN) of the mandible: a laser Raman spectroscopic study. Appl. Spectros. **57**:1100-1116.

43. Ager III JW, R. K. Nalla RK, Breeden KL, Ritchie RO 2005 Deep-ultraviolet Raman spectroscopy study of the effect of aging on human cortical bone. J Biomed Opt. **10**:034012.

44. Marshall Jr GW, Yücel N, Balooch M, Kinney JH, Habelitz S, Marshall SJ 2001 Sodium hypochlorite alterations of dentin and dentin collagen. Surf Sci **491**:444-455.

45. Jenness DD, Sprecher C, Johnson Jr WC 1976 Circular dichroism of collagen, gelatin, and poly(proline) II in the vacuum ultraviolet. Biopolymers **15**: 513-521.

46. Wang Y-N, Galiotis C, Bader DL 2000 Determination of molecular changes in soft tissues under strain using laser Raman microscopy. J Biomech **33**:483-486.

47. Kinney JH, Habelitz S, Marshal Jr GW, unpublished SAXS and visible Raman spectroscopy results.

48. Weiner S, Wagner, HD 1998 The material bone: structure-mechanical function relations. Ann Rev Mater Sci **28**:271-298.

49. Kanca, J 1992 Improving bond strength through acid etching of dentin and bonding to wet dentin surfaces. J Am Dent Assoc **123**:35-43.

50. Marshall Jr GW, Marshall SJ, Kinney JH, Balooch M 1997 The dentin substrate: structure and properties related to bonding. J Dent **25**:441-58.

51. Marshall Jr GW, Wu-Magid IC, Watanabe LG, Inai N, Balooch M, Kinney JH, Marshall SJ 1998 Effect of citric acid concentration on dentin demineralization, dehydration, and rehydration: atomic force microscopy study. J Biomed Mater Res **42**:500-7.

52. Kinney JH, Balooch M, Marshall GW, Marshall, SJ 1999 A micromechanics model of the elastic properties of human dentine. Arch Oral Biol **44**:813-22.

53. Zheng L, Hilton, JF, Habelitz S, Marshall SJ, Marshall, GW 2003 Dentin caries activity status related to hardness and elasticity. Eur J Oral Sci **111**:243-52.

54. Angker L, Nijhof N, Swain MV, Kilpatrick, NM 2004 Influence of hydration and mechanical characterization of carious primary dentine using an ultra-micro indentation system (UMIS). Eur J Oral Sci **112**:231-6.

55. Habelitz S, Balooch, M, Marshall, SJ, Balooch G, Marshall, GW 2002 *In situ* atomic force microscopy of partially demineralized human dentin collagen fibrils. J Struct Biol **138**:227-36.

56. Bella J, Brodsky B, Berman HM 1995 Hydration structure of a collagen peptide. Structure **3**:893-906.

57. Price RI, Lees S, Kirschner, DA 1997 X-ray diffraction analysis of tendon collagen at ambient and cryogenic temperatures: role of hydration. Int J Biol Macromol **20**:23-33.

58. Orgel JP, Wess TJ, Miller A. 2000. The in situ conformation and axial location of the intermolecular cross-linked non-helical telopeptides of type I collagen. Structure **8**:137-42.

59. Wilson EE, Awonusi A, Morris MD, Kohn DH, Tecklenburg MMJ, Beck LW 2005 Highly ordered interstitial water observed in bone by nuclear magnetic resonance. J Bone Min Res **20**:625-634.

60. Nalla RK, Balooch M, Ager III, JW, Kruzic JJ, Kinney JH, Ritchie RO 2005 Effects of polar solvents on the fracture resistance of dentin: role of water hydration. Acta Biomaterialia **1**:31-43.

61. Kiebzak GM 1991 Age-related bone changes. Exp Gerontol. **26**:171-187.

62. Parfitt AM 1988 Bone remodeling: relationship to the amount and structure of bone, and the pathogenesis and prevention of fractures. In: B. L. Riggs and L. J. Melton, editors Osteoporosis: Etiology, Diagnosis, and Management. Raven Press, New York, USA, pp. 45-94.

63. Matsushima N, Hikichi K 1989 Age changes in the crystallinity of bone mineral and in the disorder of its crystal. Biochim. Biophys. Acta **992**:155-159.

Table 1. Summary of peak assignments for the major features observed in the ultraviolet resonance Raman (UVRR) spectroscopy of human bone and dentin using an excitation wavelength of 244 nm. The instrumental limit for determining for peak positions was ±5 cm^{-1}. Minor spectroscopic features are discussed in the text.

Peak range (cm^{-1})	Assignment
955-965	PO_4^{3-} ν_1 from apatite
1245-1255	amide III from peptide bonds
1455-1465	CH_2 wag [34]
1555-1565	amide II from peptide bonds
1610-1620	Y8a (tyrosine side chain vibration)
1655-1665	amide I from peptide bonds

FIGURE CAPTIONS.

FIG. 1. UV Resonance Raman spectra excited at 244 nm from human dentin. Representative spectra from each group in the study are shown young/normal; aged/non-transparent; aged/transparent. Spectra are normalized to the intensity of the CH_2 wag feature. The spectra were obtained with a slit width corresponding to 30 cm^{-1} resolution; the precision for determining peak positions is ca. ±5 cm^{-1}.

FIG. 2. Comparison of typical UV resonance Raman spectra of proteins in mineralized tissues and in aqueous solution. (a) Human molar, 244 nm, this work. (b) hydrated gel-like type I collagen, this work. (c) Collagen in aqueous solution, 229 nm excitation, Juszczak [33]. (d) Myoglobin in aqueous solution [31]. For proteins in aqueous solution, excitation at near 230 nm (c) and near 200 nm (d) enhances scattering from the ring stretches of aromatic amino acids and the amide features, respectively. Scattering from both aromatic rings and amide feature is enhanced for 244 nm excitation for solid mineralized tissues (a). Spectra are normalized to the intensity of the CH_2 wag feature [(d) is divided by 5].

FIG. 3. Non-linear least-squares fits of the spectral region between 1400 and 1800 cm^{-1} for two of the samples in this study. Spectra are fit to four overlapping features with the indicated approximate frequencies: CH_2 wag -1460 cm^{-1}, amide II - 1550 cm^{-1}; Y8a - 1620 cm^{-1}, amide I - 1660 cm^{-1}.

FIG. 4. UVRR spectra (244 nm excitation) of young/normal dentin exposed to citric acid to induce demineralization using an exposure time between 15 sec and 24 hr: (a) demineralized dentin maintained in its hydrated state and (b) demineralized dentin allowed to dry. The relative peak heights of the phosphate peak at 960 cm^{-1}, Y8a (1610 cm^{-1}), and amide I (ca. 1660 cm^{-1}) are shown in the insets as a function of exposure time. The collapse of the dentin structure produced by demineralization and dehydration produces an increase in the amide I peak height.

FIG. 5. UVRR spectra (244 nm excitation) of dentin from the young/normal sample group exposed to citric acid for 24 hr to induce demineralization, subsequently dehydrated, and then rehydrated. The increase in the height of the overlapped Y8a/amide I feature upon dehydration is reversible.

FIG. 6. Peak heights for the Y8a and amide I feature obtained from non-linear least squares fitting of UVRR spectra (c.f. Fig. 3) obtained from (a) the dentin sample set in this work, (b) demineralized dentin, (c) human cortical bone [43]. Bars indicate standard deviations. Significant differences in means compared to the Normal group in (a), the Control group in (b), and the youngest data set in (c) are indicated as follows (t-test): * $p < 0.05$, ** $p < 0.01$ *** $p < 0.001$.

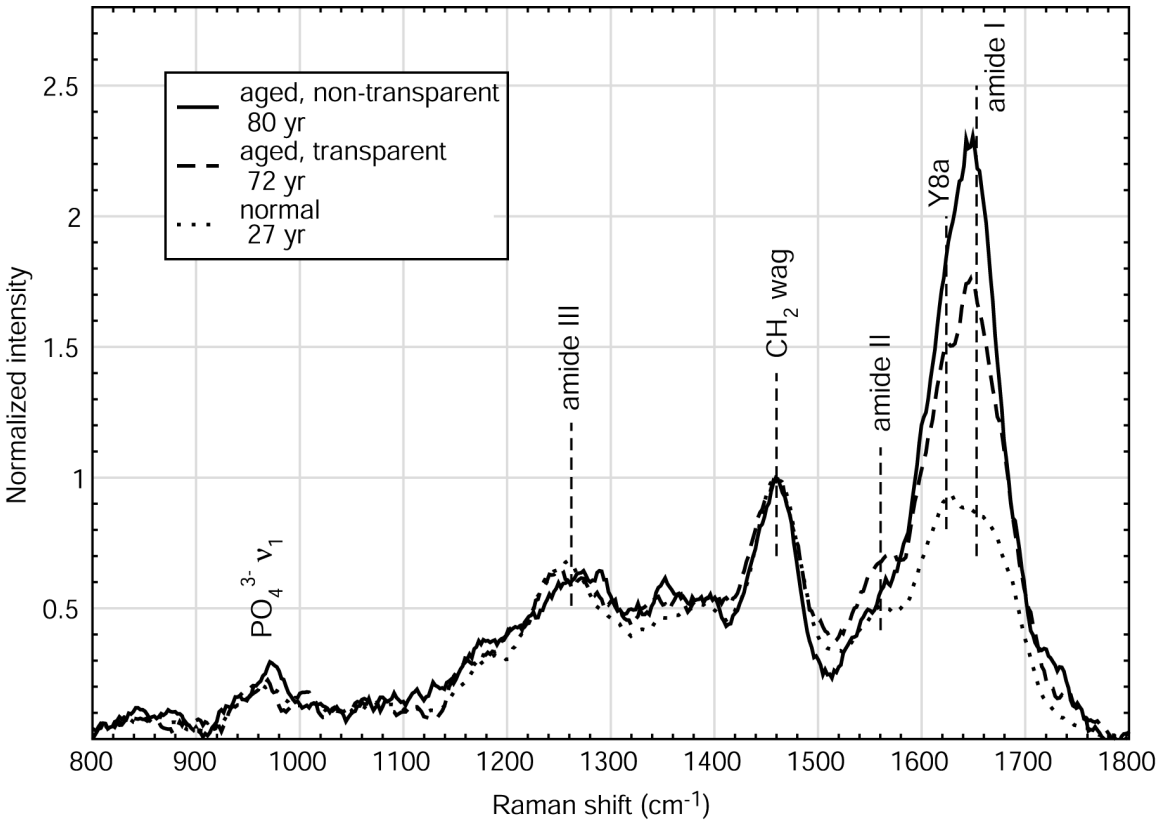

FIG. 1. UV Resonance Raman spectra excited at 244 nm from human dentin. Representative spectra from each group in the study are shown young/normal; aged/non-transparent; aged/transparent. Spectra are normalized to the intensity of the CH_2 wag feature. The spectra were obtained with a slit width corresponding to 30 cm^{-1} resolution; the precision for determining peak positions is ca. ±5 cm^{-1}.

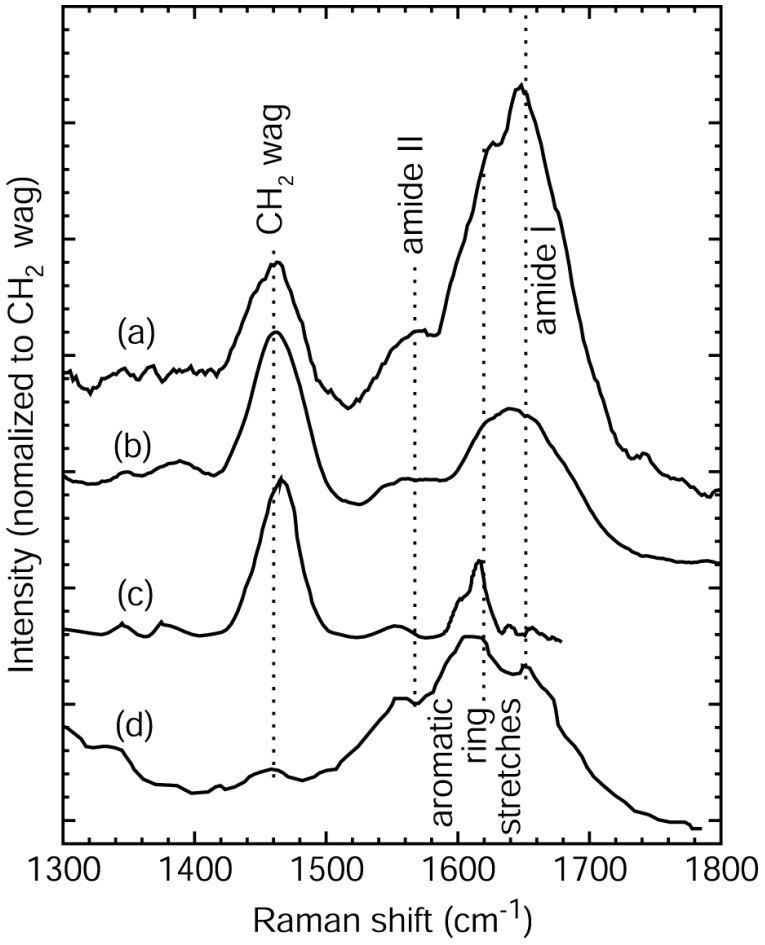

FIG. 2. Comparison of typical UV resonance Raman spectra of proteins in mineralized tissues and in aqueous solution. (a) Human molar, 244 nm, this work. (b) hydrated gel-like type I collagen, this work. (c) Collagen in aqueous solution, 229 nm excitation, Juszczak [33]. (d) Myoglobin in aqueous solution [31]. For proteins in aqueous solution, excitation at near 230 nm (c) and near 200 nm (d) enhances scattering from the ring stretches of aromatic amino acids and the amide features, respectively. Scattering from both aromatic rings and amide feature is enhanced for 244 nm excitation for solid mineralized tissues (a). Spectra are normalized to the intensity of the CH_2 wag feature [(d) is divided by 5].

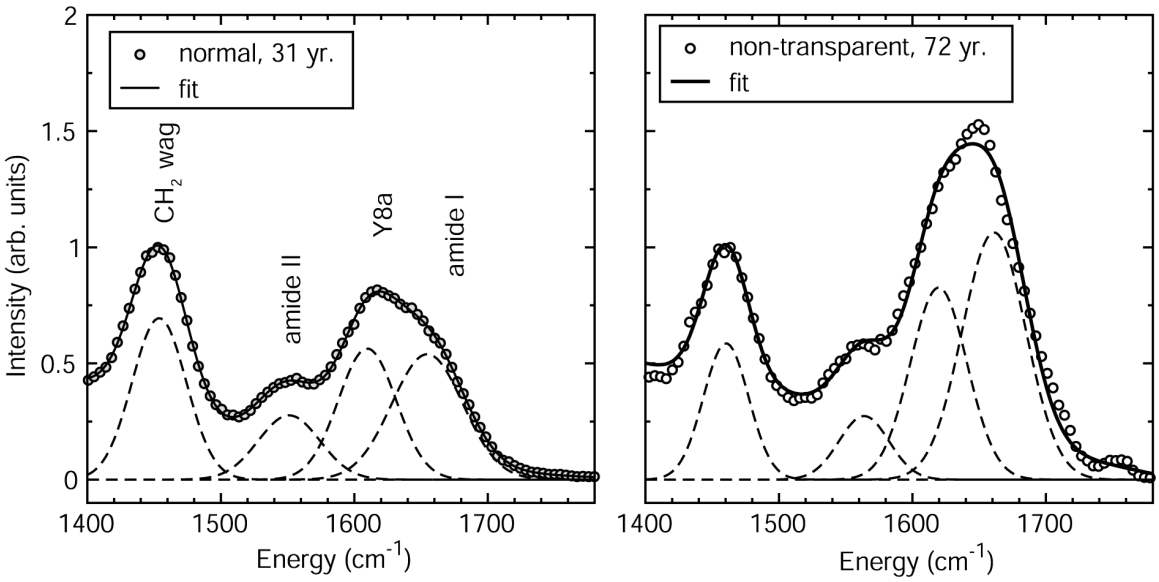

FIG. 3. Non-linear least-squares fits of the spectral region between 1400 and 1800 cm^{-1} for two of the samples in this study. Spectra are fit to four overlapping features with the indicated approximate frequencies: CH_2 wag -1460 cm^{-1}, amide II - 1550 cm^{-1}; Y8a - 1620 cm^{-1}, amide I - 1660 cm^{-1}.

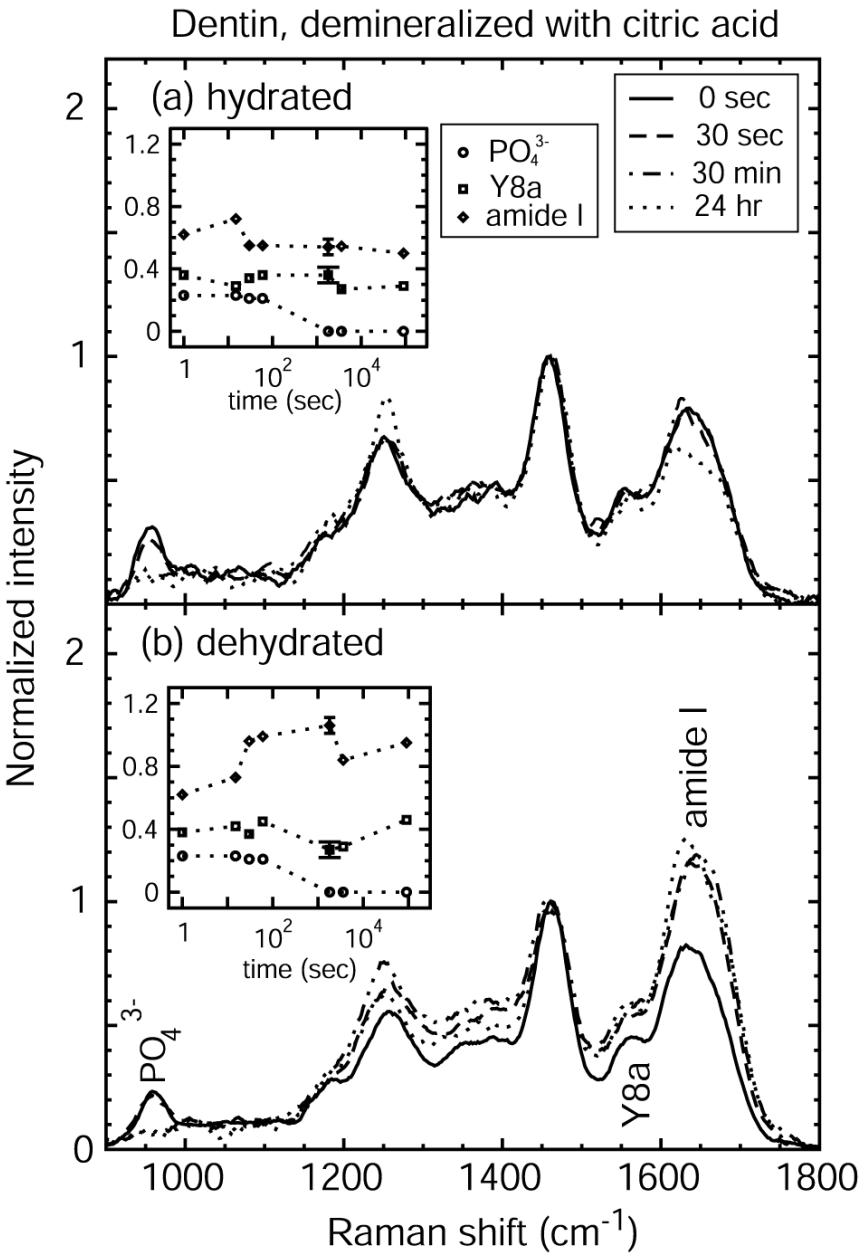

FIG. 4. UVRR spectra (244 nm excitation) of young/normal dentin exposed to citric acid to induce demineralization using an exposure time between 15 sec and 24 hr: (a) demineralized dentin maintained in its hydrated state and (b) demineralized dentin allowed to dry. The relative peak heights of the phosphate peak at 960 cm^{-1}, Y8a (1610 cm^{-1}), and amide I (ca. 1660 cm^{-1}) are shown in the insets as a function of exposure time. The collapse of the dentin structure produced by demineralization and dehydration produces an increase in the amide I peak height.

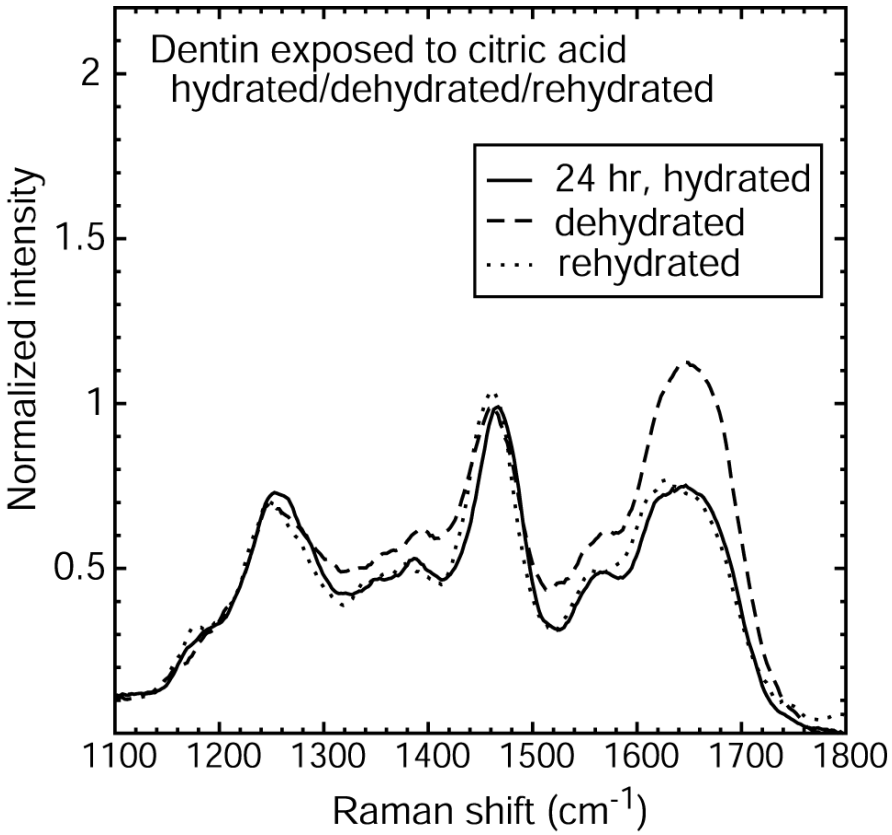

FIG. 5. UVRR spectra (244 nm excitation) of dentin from the young/normal sample group exposed to citric acid for 24 hr to induce demineralization, subsequently dehydrated, and then rehydrated. The increase in the height of the overlapped Y8a/amide I feature upon dehydration is reversible.

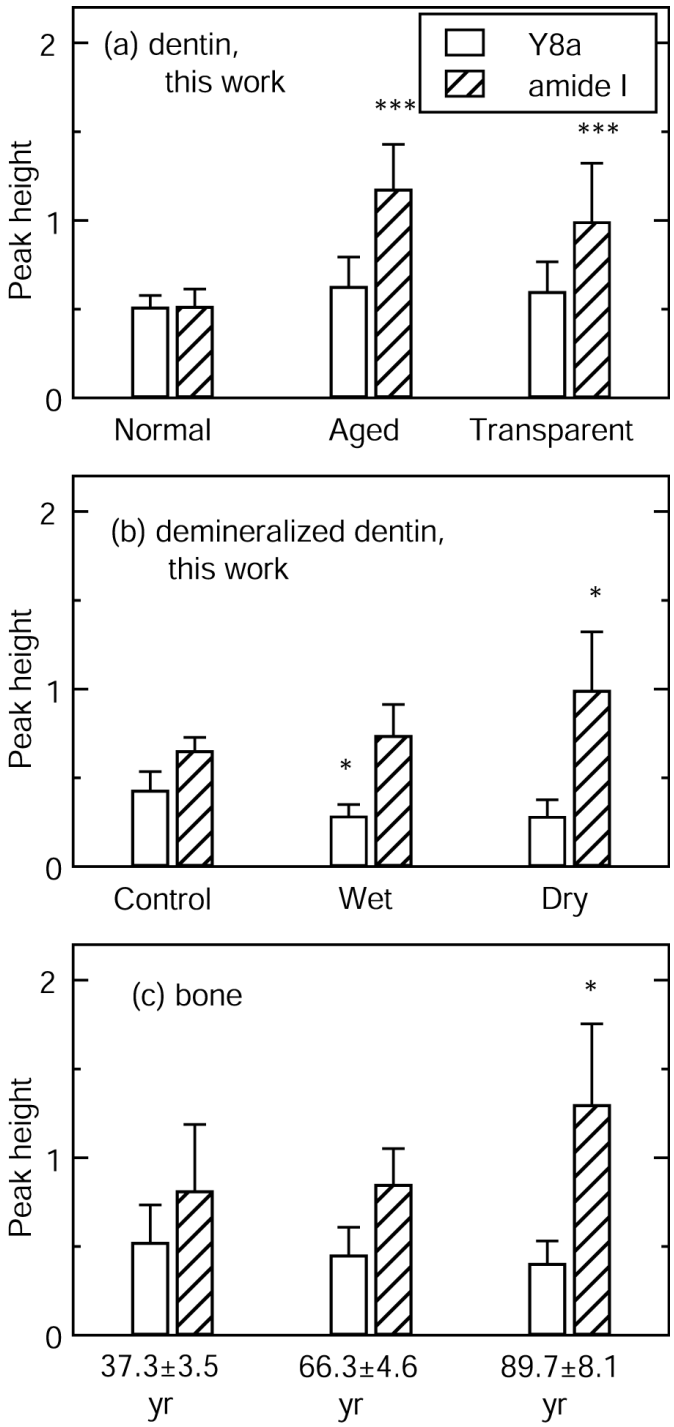

FIG. 6. Peak heights for the Y8a and amide I feature obtained from non-linear least squares fitting of UVRR spectra (c.f. Fig. 3) obtained from (a) the dentin sample set in this work, (b) demineralized dentin, (c) human cortical bone [43]. Bars indicate standard deviations. Significant differences in means compared to the Normal group in (a), the Control group in (b), and the youngest data set in (c) are indicated as follows (t-test): * $p < 0.05$, ** $p < 0.01$ *** $p < 0.001$.